# Feedback processes between magmatic events and flank movement at Mount Etna (Italy) during the 2002–2003 eruption

Thomas R. Walter,[1] Valerio Acocella,[2] Marco Neri,[3] and Falk Amelung[4]

Received 14 February 2005; revised 7 June 2005; accepted 15 July 2005; published 27 October 2005.

[1] The 2002–2003 Mount Etna eruption and the associated deformation provide a unique possibility to study the relationships between volcanism and volcano instability. The sequence started with movement of the eastern volcano flank and was associated with earthquakes and the formation of surface ruptures. Then the eruption occurred from fissures at the north and south rift zones and was followed by additional flank movement, seismic swarms, and surface ruptures. The overall area of flank movement implicated more than 700 km$^2$. In this paper we investigate how episodes of magmatic events (eruptions and intrusions) and flank movement interact. In three-dimensional numerical models we simulate the volcano-tectonic events and calculate changes in the static stress field. The models suggest that the 2002–2003 events are the result of interrelated processes consisting of (1) the preeruptive intrusion of magma and inflation of the volcano, which induced (2) the movement of the volcano east flank, (3) facilitated the eruption, and (4) led to the slip of a much larger part of the eastern and southeastern flanks. Understanding the precise interconnectivity of these processes may help to forecast the behavior during future volcanic crisis at Mount Etna, which is crucial in minimizing volcanic and seismic hazards on the highly populated eastern sector of the volcano.

**Citation:** Walter, T. R., V. Acocella, M. Neri, and F. Amelung (2005), Feedback processes between magmatic events and flank movement at Mount Etna (Italy) during the 2002–2003 eruption, *J. Geophys. Res.*, *110*, B10205, doi:10.1029/2005JB003688.

## 1. Introduction

[2] A significant hazard potential in volcanic regions is not related to eruptions, but to shallow level edifice deformation, instability, and the volcano's susceptibility to collapse [*Siebert*, 1992]. Historically documented events of volcano collapse are rare and understanding and assessing the processes involved in flank destabilization and flank movement is difficult. The few volcanoes that are identified as being structurally unstable are closely monitored. Examples include the southern flank of Kilauea (Hawaii), the northern flank of Stromboli (Aeolian Islands), the eastern flank of Piton de la Fournaise (Reunion Island), and the eastern flank of Mount Etna (Sicily) [see *Borgia et al.*, 2000, and references therein]. Several studies suggest that eruptions/intrusions, flank movement and flank earthquakes are related [e.g., *Voight et al.*, 1981; *Dieterich*, 1988] and that flank movement influences magma propagation and the geometry of intrusive rift zones [e.g., *Walter et al.*, 2005]. If there is a positive feedback between these processes, we might use precursory stages of unrest as a tool to assess the potential of flank movement and of volcanic activity.

[3] In this paper we study the possible feedback process between flank movement and volcanic activity for Mount Etna Volcano, Italy. The occurrence of such feedback processes is likely to be linked to eruptive cycles at Mount Etna. A typical eruptive cycle consists of three distinct phases [after *Behncke and Neri*, 2003]: phase I, a period of eruptive quiescence lasting <3.5 years; phase II, a period of relatively continuous summit eruptions lasting 6 to 16 years; and phase III, a series of flank eruptions with intervening summit eruptions lasting 9 to 22 years. The most recent eruptive cycle of Mount Etna started in 1993. Phase I lasted from 1993 to 1995, phase II from 1995 to 2001, and phase III started with a fissure eruption in 2001, and includes the 2002–2003 eruptions. Associated with phase III was a significant displacement of the eastern flank of Mount Etna. The 2002–2003 events suggest that flank movement temporally correlates with eruptive and fumarole activity [*Acocella et al.*, 2003; *Burton et al.*, 2004; *Neri et al.*, 2005]. However, a detailed study of the mechanism of interaction between volcanism and flank movement was not performed prior to this study.

[4] We use numerical elastic models to simulate stress changes associated with the magmatic events and flank movement at Mount Etna. Our models suggest that magma injection increases the Coulomb failure stress at active faults and encourages fault slip. Slip at these faults in turn alters the stress and pressure conditions at the magmatic system.

[1] GeoForschungsZentrum Potsdam, Potsdam, Germany.
[2] Dipartimento di Scienze Geologiche, Università di Roma TRE, Rome, Italy.
[3] Istituto Nazionale di Geofisica e Vulcanologia, Catania, Italy.
[4] Marine Geology and Geophysics Division, Rosenstiel School of Marine and Atmospheric Science, University of Miami, Miami, Florida, USA.


0148-0227/05/2005JB003688$09.00

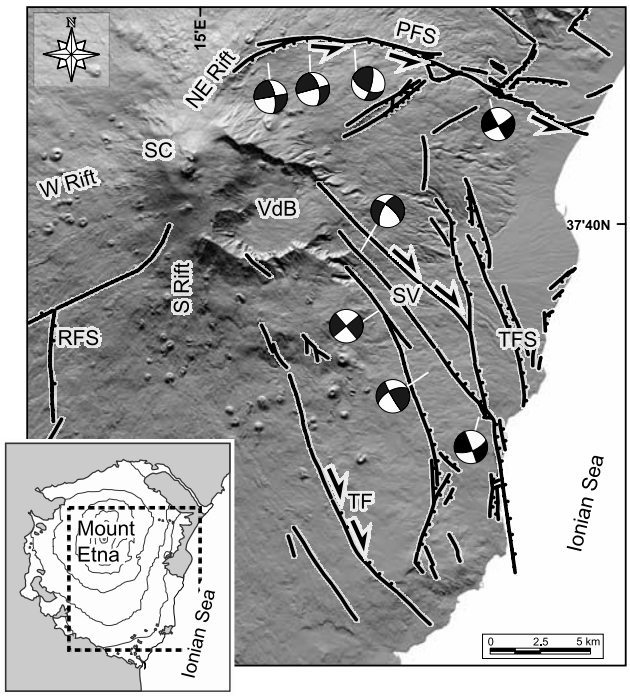


**Figure 1.** Shaded relief map of Mount Etna (the area shown is indicated by the dashed box in the lower left inset). Black solid lines trace the main faults on the edifice. PFS, Pernicana Fault System; SV, Santa Venerina Fault; TFS, Timpe Fault System; TF, Trecastagni Fault; RFS, Ragalna Fault System. The main intrusive axes are the NE rift and the south rift; a lesser active third rift arm is the west rift. SC, Summit Craters; VdB, Valle del Bove. Focal mechanisms are after *Gambino et al.* [2004] and *Neri et al.* [2005].

A detailed stress change analysis may help to assess coming stages of eruptions and the potential for sudden flank displacements at Mount Etna.

## 2. Geology of Mount Etna

[5] Mount Etna is located in eastern Sicily, along the Malta escarpment at the front of the Apennine-Maghrebian Chain. The structural evolution of the edifice is influenced by the regional tectonic setting and by local-scale volcano-tectonic processes [see, e.g., *Lo Giudice et al.*, 1982; *McGuire et al.*, 1990; *Corsaro et al.*, 2002; *Branca et al.*, 2004; *Azzaro*, 2004]. In the following, we focus on the local processes at the volcano, i.e., volcanic activity and flank instability.

### 2.1. Volcanic Activity

[6] Volcanism in the initial stages of growth of Mount Etna was in part submarine and not centralized [*Corsaro et al.*, 2002]. The evolution of Mount Etna included phases of shield building, nesting of volcanic centers and calderas, and the final constructional phase of the stratovolcano [*Branca et al.*, 2004]. The present Mount Etna edifice is ~35 km wide and more than 3300 m high (Figure 1). Recent eruptions of Mount Etna are characterized by summit eruptions at the 4 central craters, and by fissure eruptions and dike intrusions at the rift zones oriented NE, south and west [*Behncke and Neri*, 2003]. During the last 400 years, ~50% of the eruptions occurred along the rift zones through fissures opened on the volcano flanks [*Behncke et al.*, 2005]. These fissures are usually related to the lateral intrusion of dikes radiating from a shallow magma conduit system (central lateral fissures). In rare cases, magma bypasses the central magma conduit system and propagates directly from deeper levels into the rift zones (eccentric eruptions, according to *Acocella and Neri* [2003]). The 2002–2003 eruption was associated with simultaneous central lateral and eccentric fissures [*Neri et al.*, 2005].

[7] The position and dimension of a shallow magmatic reservoir system below Mount Etna is subject to debates. Recent geodetic data (GPS, interferometric synthetic aperture radar) suggest that a shallow reservoir is located at ~3–4 km depth [*Puglisi et al.*, 2001; *Bonforte and Puglisi*, 2003; *Lundgren et al.*, 2003]. However, the presence of earthquakes and the lack of a zone of seismic quiescence at this level imply that this reservoir is rather small [*Neri et al.*, 2005]. Seismic data suggest that a larger magma body is located at 4–6 km depth or at greater depth [*Murru et al.*, 1999; *Patanè et al.*, 2003; *Neri et al.*, 2005].

### 2.2. Flank Instability

[8] The edifice of Mount Etna is subject to lateral spreading, mostly on its eastern flanks [*Borgia et al.*, 1992] and to a lesser degree also on its western flanks [*Lundgren et al.*, 2004]. In the following, we focus on processes of flank movement at the unstable eastern flank.

[9] The upper eastern flank of Mount Etna exhibits the Valle del Bove, which is probably the embayment of a shallow lateral collapse and subsequent erosion (VdB in Figure 1, a >5-km-wide and >8-km-long scar with about 30 km$^2$ [*Borgia et al.*, 1992; *Tibaldi and Groppelli*, 2002; *Calvari et al.*, 2004]). The unstable eastern flank though is much larger than the collapse scar of the Valle del Bove and involves most of the eastern and southern flanks of Mount Etna (Figure 1) [e.g., *Borgia et al.*, 1992; *Rust and Neri*, 1996] and is framed by the E-W striking sinistral transtensive Pernicana Fault System (PFS in Figure 1) and the N-S striking transtensive dextral Ragalna Fault System (RFS in Figure 1) [e.g., *Rust and Neri*, 1996; *Neri et al.*, 2004; *Acocella and Neri*, 2005]. A subhorizontal detachment plane, hereinafter referred to as the "decollement," lies beneath the east flank at a depth of about 5 km below sea level (bsl). The decollement has been inferred by different sets of data such as field evidence, the distribution of seismicity and surface deformation, and the deformation pattern observed during east flank movement [e.g., *Borgia et al.*, 1992, 2000; *Acocella et al.*, 2003; *Neri et al.*, 2004; *Lundgren et al.*, 2004], suggesting a thrust-type fault plane with a slight (5–10°) westward dip. An additional detachment plane may be located at shallower depths (~2–3 km bsl), with a slight eastward dip [*Puglisi et al.*, 2001; *Tibaldi and Groppelli*, 2002; *Bonforte and Puglisi*, 2003; *Lundgren et al.*, 2003, 2004]. Similar decollement planes at the base of a volcano are known elsewhere and considered to be the result of gravitational

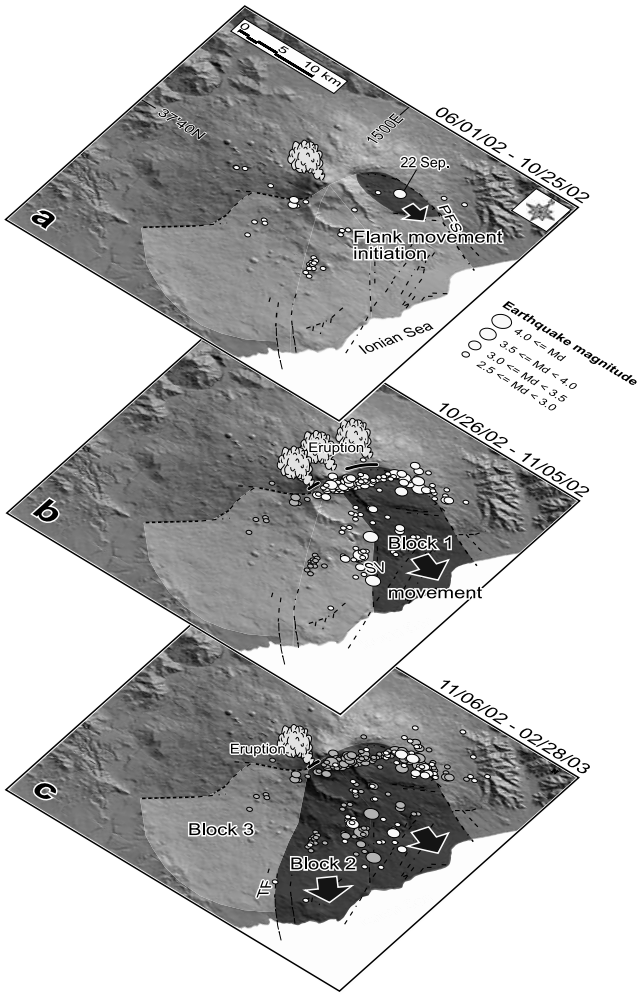


**Figure 2.** Perspective view of Mount Etna looking to the NW, showing distribution of seismicity and propagation of flank movement in three time frames, between 1 June 2002 and 28 February 2003 (modified according to *Acocella et al.* [2003] and *Neri et al.* [2005]). Earthquakes during each time frame are shown by white circles. Dark shaded region corresponds to the unstable eastern flank of Mount Etna during the time frame. Faults and acronyms are same as in Figure 1.

stresses, weak substrata and forceful intrusions [*Borgia et al.*, 2000].

### 2.3. Volcanic Activity and Flank Instability in 2002–2003

[10] Prior to the 2002–2003 events, inflation of shallow magma pockets under Mount Etna was detected, probably as a result of the arrival of new magma [*Patanè et al.*, 2003, and references therein]. The source location of inflation was between 4 and 6 km depth bsl [*Patanè et al.*, 2003; *Neri et al.*, 2005]. In 2002–2003 the volcano became very active, with fissure eruptions at the rift zones and significant flank movement [e.g., *Aloisi et al.*, 2003; *Bonforte and Puglisi*, 2003; *Lundgren et al.*, 2003, 2004].

[11] The 2002–2003 unrest started with a seismic swarm along the westernmost Pernicana Fault. Earthquakes related to this displacement were of small magnitude (for instance, a main shock had *M*3.7 on 22 September 2002). Although most of the slip occurred without large earthquakes, abundant E-W fractures formed at the surface and the associated destruction of walls and roads was substantial.

[12] The main eruption started about one month later on 26 October 2002, forming eruptive fissures along the NE and the south rifts that were active for 7 days and 3 months, respectively. Immediately after the onset of the eruption, the Pernicana Fault moved again and the surface fractures propagated seaward. The length of the active Pernicana Fault increased to ~20 km. The cumulative displacement reached more than 120 cm, which, for a fault width of 3–5 km, corresponds to a moment release equivalent to an earthquake with magnitude *M*5.8 to *M*6.0 ($M_0$ = 6–10 × $10^{24}$ dyn/cm).

[13] Subsequent seismic swarms occurred on two other fault zones. On 29 October 2002, a seismic swarm with surface fracturing (NNW-SSE right-lateral transtensive strike-slip faults) affected the Santa Venerina Fault zone (SV, Figure 2). On 26 November 2002, another seismic swarm with surface fracturing (NNW-SSE right-lateral transtensive strike-slip faults) affected the Trecastagni Fault zone (TF, Figure 2). The distributions of seismicity and the associated focal mechanisms in this time period are consistent with the formation, location and kinematics of surface ruptures.

[14] During the following 2 years (2003–2004), the Ragalna Fault zone (RFS, Figure 2) showed ~6 cm of displacement. The time delay of the Ragalna Fault slip, however, suggests that the displacement is not directly related to the volcanic events.

[15] On the basis of earthquake swarms, fault displacements and the temporal evolution of flank instability during this 2002–2003 sequence, *Acocella et al.* [2003] and *Neri et al.* [2004] proposed a block model for the unstable eastern sector of Mount Etna and distinguished three major structural blocks (Figure 2). The boundaries between the three blocks match the Santa Venerina Fault (SV, between blocks 1 and 2) and the Trecastagni Fault (TF, between blocks 2 and 3). The displaced flank involved a total area of about 700 km$^2$, with block 1 ≈ 210 km$^2$, block 2 ≈ 155 km$^2$ and block 3 ≈ 335 km$^2$ (Figure 2). The displaced submarine part of the flank is not known and may increase this figure substantially. Estimation of the volume of the displaced flank is also difficult because of the poorly constrained depth of the basal decollement under the three blocks. A decollement at sea level gives the minimum displaced volume estimate with about 500 km$^3$. For a decollement at 2 km below sea level, the total displaced volume would be about 2,000 km$^3$. For a decollement at 5 km below sea level, which is the depth constrained by earthquake locations [*Neri et al.*, 2005], the displaced volume is even much higher. The dimension of the displaced eastern flank of Mount Etna is therefore comparable to the dimension of giant landslides previously known only for ocean island volcanoes. The sequential movement of blocks 1, 2, and 3 and the simultaneous occurrence of earthquake swarms, surface fractures and eruptions, suggests that these processes interacted during the 2002–2003 sequence. In the following we test whether

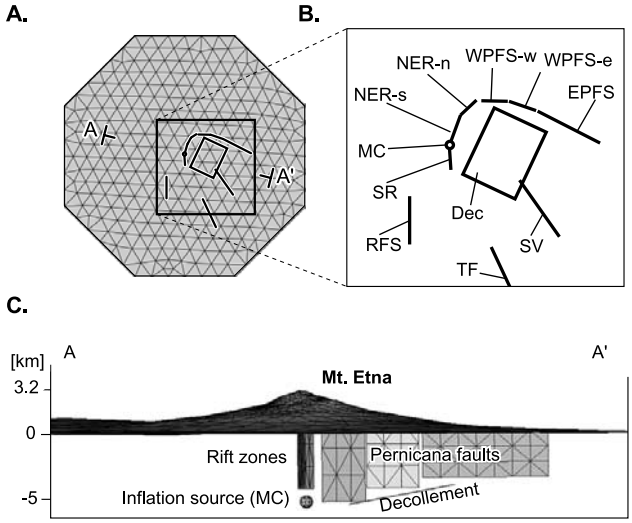


**Figure 3.** Map view of the boundary element model geometry, showing (a) the topographic mesh and (b) the dislocation sources considered in this paper. The topographic mesh (here resampled for illustration) was traction free and located in isotropic elastic full space. (c) The dislocation sources underneath were a sphere (shallow reservoir), vertical rectangular planes (rift zones and strike-slip faults), and the 10° westward dipping plane (decollement). The results were calculated in the cross section parallel to the main faults or rift zones, except for the decollement (perpendicular section). The faults and rift zones were modeled in segments that allow curved geometries or variable slip, i.e., three segments for PFS, two for NER; otherwise acronyms are the same as in Figure 1.

the temporal sequence of events is consistent with changes of the static stress field.

## 3. Static Stress Changes

[16] Static stress changes play an important role in the occurrence of earthquakes [e.g., *Stein*, 1999] or eruptions [e.g., *Hill et al.*, 2002]. Volcanic eruptions can be influenced or even triggered by stress changes caused by fault displacement, and earthquakes tend to occur on faults that have experienced an increase in Coulomb stress by previous events [e.g., *Thatcher and Savage*, 1982; *Harris*, 1998; *Nostro et al.*, 1998; *Stein*, 1999; *Hill et al.*, 2002; *Marzocchi et al.*, 2002; *Walter and Amelung*, 2004]. The magnitude of static stress changes during eruptions or earthquakes is typically on the order of 0.1–10 bars [*Hill et al.*, 2002]. Tidal triggering of earthquakes by stress changes of about 0.01 bar was recently documented [*Tanaka et al.*, 2004].

[17] We will now study static stress changes associated with the 2002–2003 Mount Etna scenarios. Our numerical models may help to understand the interaction between magmatic emplacement and eruptions at Etna and the movement of its eastern flank. We examine how (1) intrusions and eruptive dikes in the edifice influence the stress along faults on the eastern flank (section 4.1) and how (2) fault displacements on the eastern flank interact and encourage volcanic eruptions (section 4.2).

### 3.1. Modeling Method and Setup

[18] We use a modified version of Poly3D [*Thomas*, 1993], a three-dimensional boundary element (BEM) program that is based on the theory of linear elasticity [*Crouch and Starfield*, 1983; *Becker*, 1992]. Within the isotropic media, the analytical equations for triangular dislocation sources are solved [*Comninou and Dundurs*, 1975]. With planar, polygonal elements of displacement discontinuity, Poly3D calculates quasi-static displacements, strain, and stress fields. The displacement discontinuity is decomposed into three components where the component normal to the element plane may represent a dike opening, while the other two components parallel to the plane represent strike-slip or dip-slip dislocation.

[19] Surface topography, dikes, a magma reservoir, and the faults are represented as objects that consist of collections of triangular dislocation elements (see Figure 3). The geometry of these objects (Table 1) derives from geological and geophysical data [e.g., *Patanè et al.*, 2003; *Branca et al.*, 2003; *Aloisi et al.*, 2003; *Lundgren et al.*, 2003, 2004; *Neri et al.*, 2004, 2005]. For these objects, traction or dislocation boundary conditions were defined to simulate the following:

#### 3.1.1. Effect of the Topography

[20] The free surface is traction-free and therefore affects the distribution of stresses, strains and displacements in the

**Table 1.** Geometries Imposed in the Models[a]

| Intrusion Model | Abbreviation | UTM Position Start | UTM Position End | Fault Depth, km | Strike, deg | Dip, deg | Slip Direction | Loading |
|---|---|---|---|---|---|---|---|---|
| Reservoir inflation | MC | 498.7/4178.2 | 500.7/4178.2 | −4.0 to −6.0 | ND | ND | overpressure | 12 MPa |
| NE rift zone dike, southern segment | NER-s | 499.7/4179.2 | 501.1/4181.5 | +3.0 to −4.0 | 25 | 90 | opening | 2 m |
| NE rift zone dike, northern segment | NER-n | 501.1/4181.5 | 503.6/4184.7 | +2.3 to −4.0 | 35 | 90 | opening | 2 m |
| South rift zone dike | SR | 499.7/4177.2 | 500.3/4174.2 | +3.0 to −4.0 | 170 | 90 | opening | 1 m |
| Western Pernicana Fault System, western segment | WPFS-w | 504.5/4183.9 | 507.4/4183.9 | +2.0 to −5.0 | 90 | 90 | left lateral | 1.25 m |
| Western Pernicana Fault System, eastern segment | WPFS-e | 507.4/4183.9 | 512.5/4182.4 | +1.7 to −4.0 | 105 | 90 | left lateral | 0.5 m |
| Eastern Pernicana Fault System | E PFS | 512.5/4182.4 | 521.3/4179.5 | +1.3 to −3.0 | 110 | 90 | left lateral | 0.1 m |
| Santa Venerina | SV | 509.3/4174.2 | 515.0/4165.6 | +0.5 to −5.0 | 145 | 90 | right lateral | 0.2 m |
| Ragalna Fault System | RFS | 492.7/4171.1 | 492.6/4165.2 | +1.3 to −4.0 | 180 | 90 | right lateral | ND |
| Trecastagni Fault | TF | 505.6/4165.4 | 510.0/4156.2 | +0.6 to −4 | 155 | 90 | right lateral | ND |
| Décollement fault | Dec | 501.8/4176.0 | 513.2/4181.8 | −5.1 to −3.8 | 25 | −10 | thrust fault | 1 m |

[a]The length of a dislocation source is given by the coordinates, where the start is the lower left corner of a dislocation source and the end is the upper right corner. The depth of a dislocation source is defined by the sea level (0) and the free surface (upper limit, positive value) and the depth below the sea level (negative value). ND indicates not determined.

upper crust. Because the earth's surface can be treated as a traction-free boundary, we can consider the topographic effect by simulating a free surface. The Mount Etna topography was meshed by triangulating the 90-m Shuttle Radar Topography Mission data into 1200 elements. At each element we defined the boundary conditions so that it acted as a traction-free boundary in an elastic full space.

#### 3.1.2. Displacement at the Faults

[21] The geometry of the faults is based on recent geological and geophysical studies at Mount Etna [*Rust and Neri*, 1996; *Acocella and Neri*, 2003; *Acocella et al.*, 2003, *Neri et al.*, 2004, 2005]. We approximated the faults via linear rectangular planes of discontinuities triangulated into a 0.4-km grid. At each element of the fault we defined the boundary conditions so that it simulated uniform displacement. The amount of slip we defined was based upon observational values of the 2002–2003 eruptive period at Mount Etna (see Table 1, after *Acocella et al.* [2003] and *Neri et al.* [2004]).

[22] The Pernicana Fault System is defined in our models by three segments of left-lateral faults, striking 090°, 105°, and 110°, respectively (see Table 1). Each of these segments is described by a vertical rectangular dislocation plane reaching from the free surface down to depths of 3–5 km bsl (see also Figure 3). Dislocation is uniform, being largest at the westernmost segment (1.25 m) and smallest at the eastern segment (0.1 m) [*Neri et al.*, 2004].

[23] The modeled decollement has a rectangular dimension. Empirical values regarding the real amount of slip at this decollement do not exist and we assume 1 m of slip (the mean slip observed at the surface during 2002–2003 [*Acocella et al.*, 2003]).

#### 3.1.3. Opening of Dikes

[24] Dike intrusions were modeled by rectangular planes of discontinuities with tensile dislocation boundary conditions. We defined the element conditions of a dike to be a uniform element-normal displacement discontinuity. The geometry of the dikes used in this study is based on values published by *Neri et al.* [2004, 2005]. In order to simulate the curved geometry, we defined three segments, with the orientations 175°, 015°, and 030°, from south to north respectively. The location of the model dike is given in Table 1; the width is up to 7 km (from the free surface at 3 km height to a depth of 4 km below sea level). We use a uniform widening of the dikes of 1 m (for the southern dike segment) and 2 m (for the northern segments).

#### 3.1.4. Magma Accumulation in a Reservoir

[25] A spherical balloon constructed by 120 triangular elements simulates a reservoir 2 km in diameter from 4 to 6 km depth, which is in agreement with recent geophysical data [*Puglisi et al.*, 2001; *Bonforte and Puglisi*, 2003; *Lundgren et al.*, 2003; *Neri et al.*, 2005]. An increase of the magma overpressure perturbs the stress field in the surrounding crust. Using positive tractional boundary conditions normal to the element we define an overpressure of 12 MPa, a value that is realistic for moderately inflating magma bodies. The location of the reservoir was centered under the edifice center.

[26] We assign a Poisson's ratio of $\nu = 0.25$ and a Young's modulus of $E = 70$ GPa. If not otherwise stated, the results are shown in cross sections with the model volcano oriented parallel to the known fault traces.

#### 3.1.5. Simplifications

[27] The surface traces of the faults are visible, well mapped and constrained. The amount of dislocation as modeled in this study, however, is based upon surface fractures and may differ at depth. We simplified the fault characteristics by assuming a planar strike and dip, a uniform rake, and rectangular dislocation plane geometries. For the Santa Venerina Fault, Trecastagni Fault, and Pernicana Fault we assume strike slip, neglecting a minor tensile movement [*Acocella and Neri*, 2005]. We did not simulate displacement or stress changes at the Timpe Fault System (TFS; Figure 1) because of the more regional, rather than local tectonic, character of this fault and because the displacements during the 2002–2003 sequence were insignificant. We have no factual data for the displacement at the decollement fault plane; these specific results should therefore be considered qualitatively. Mechanical heterogeneities due to e.g., thermal structure, a hydrothermal altered volcanic core or a mechanically stiff basement are not taken into account by our models.

### 3.2. Stress Field Output

[28] We consider stress changes at the faults and at the active rift zones. To study if fault slip is encouraged or discouraged, we calculate the change in Coulomb failure stress ($\Delta\sigma_C$) on receiver faults by $\Delta\sigma_C = \Delta\tau_R + \mu\,(\Delta\sigma_N + \Delta P)$, where $\Delta\tau_R$ is the change in shear stress on the receiver fault plane in the expected rake (slip) direction, $\mu$ is the coefficient of friction, $\Delta\sigma_N$ is the stress change normal to the receiver fault plane, and $\Delta P$ the pore pressure change in the fault zone [e.g., *Harris*, 1998]. Assuming undrained conditions, the pore pressure change $\Delta P$ is defined by $\Delta P = B\Delta\sigma_M$, the parameter $B$ is the Skempton's coefficient for which experimental determinations indicate $0.5 < B < 0.9$ (we use $B = 0.7$), and $\Delta\sigma_M$ is the change in mean stress [*Roeloffs*, 1996; *Beeler et al.*, 2000].

[29] Fault slip is encouraged if the change in Coulomb failure stress is positive, and discouraged if the change in Coulomb failure stress is negative. A change of the Coulomb failure stress by >1 bar is considered to be significant (note that stress triggering may occur even below 0.1 bar [see *Hill et al.*, 2002]).

[30] To determine if dike intrusions are encouraged, we calculate the change of the normal stress $\Delta\sigma_N$. Unclamping of a rift zone (positive $\Delta\sigma_N$) may facilitate the ascent of new magma and dike injection. To determine if eruptions are encouraged we calculate the change in the mean stress. Decompression of a magma reservoir may lead to the formation and ascent of bubbles, increasing the magma overpressure. A more detailed discussion of the effects of stress changes on the magmatic system follows in section 5.

## 4. Modeling Results

[31] For each model, the results are given in six cross sections parallel to the investigated fault and dike traces; only for the decollement we illustrate the results in a cross section perpendicular to the fault. We show (1) the change of the normal stress $\Delta\sigma_N$ along the rift zones, (2) the change of the Coulomb failure stress for left-lateral strike-slip faulting at the Pernicana Fault, (3) the change of the

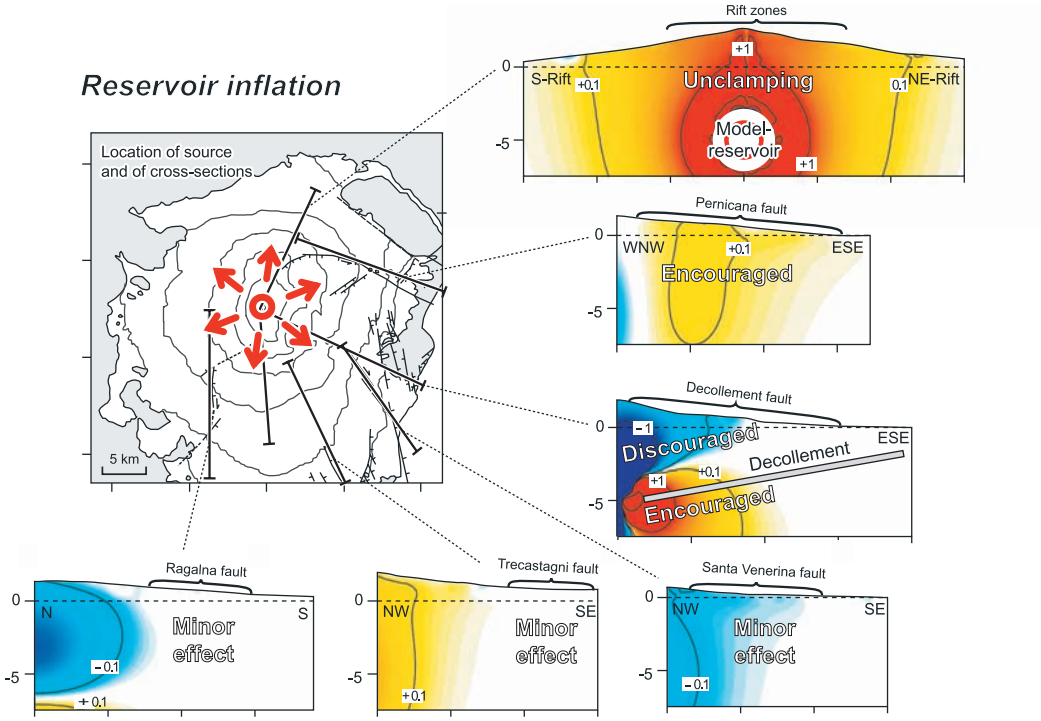


**Figure 4.** Stress changes due to magma intrusion events at Mount Etna: Preeruptive inflation. Plan view map shows the location of the loading mechanisms and of the six cross sections. Modeling results in the cross sections in a clockwise order are (1) parallel to the rift zones, (2) parallel to the Pernicana Fault, (3) perpendicular to the decollement, (4) parallel to the Santa Venerina Fault, (5) parallel to the Trecastagni Fault, and (6) parallel to the Ragalna Fault. We calculated the dike normal stress along the rift zones, suggesting unclamping for positive values (reds). All other cross sections show Coulomb failure stress change, suggesting encouraged fault displacement for positive values (reds) and discouraged faulting for negative values (blues). Brackets above each cross section indicate the approximate location of the active faults.

Coulomb failure stress for decollement thrust-type faults, (4) the change of the Coulomb failure stress for right-lateral strike-slip faulting at the Santa Venerina and Trecastagni faults, and (5) the change of the Coulomb failure stress for normal faulting at the Ragalna faults. The location, strike, dip, and rake of the faults and magmatic sources are given in Table 1. To study the effect of flank movement on the magma reservoir we then examine changes of the mean stress in a profile under the summit of the volcano.

### 4.1. Effects of Magmatic Events on Flank Movement

#### 4.1.1. Reservoir Inflation

[32] We first consider stress changes associated with reservoir inflation (Figure 4). The models show an increase of the normal stress along the rift zones (unclamping), favoring dike intrusion. We see an increase in Coulomb failure stress at the Pernicana Fault System, most significant at the shallow central and western part. For the decollement fault we see an increase of the Coulomb failure stress at depth below 3–4 km bsl. Slip along a decollement at depth of the volcano base is encouraged. Slip along a decollement at shallower depth [e.g., *Lundgren et al.*, 2003] is discouraged (Coulomb failure stress decrease). The amplitude of stress changes rapidly declines radially, which means that the decollement further to the north or south receives a significant smaller increase of Coulomb failure stress. The Santa Venerina Fault, the Trecastagni Fault, and the Ragalna Fault experience minor changes of the Coulomb failure stress, being slightly positive (TF) or slightly negative (RF, SV).

[33] In summary, shallow crustal reservoir inflation encourages dike intrusion into the rift zones, flank movement along the western Pernicana Fault System and along the deeper portion of the decollement.

#### 4.1.2. Dike Intrusion

[34] Intrusion of dikes into the rift zones causes significant stress changes within the east flank of Mount Etna (Figure 5). The cross section along the rift zones shows the extent of the model dike. The models show a significant increase of the Coulomb failure stress at the Pernicana Fault (>10 bars at the western end). In fact, the western Pernicana Fault was indeed the location of maximum fault slip during the event associated with the 2002 dike intrusion. For the decollement we see an increase of the Coulomb failure stress by >10 bars in the area of the proposed decollement at 5 km bsl. The maximum stress increase is approximately located at the depth of the lower limit of the simulated dikes. The Santa Venerina Fault experiences a Coulomb failure stress decrease; it is locked. The Trecastagni Fault at the southeastern flank of Mount Etna experiences an increase in Coulomb failure stress (<2 bar). The Ragalna Fault experiences a slight Coulomb

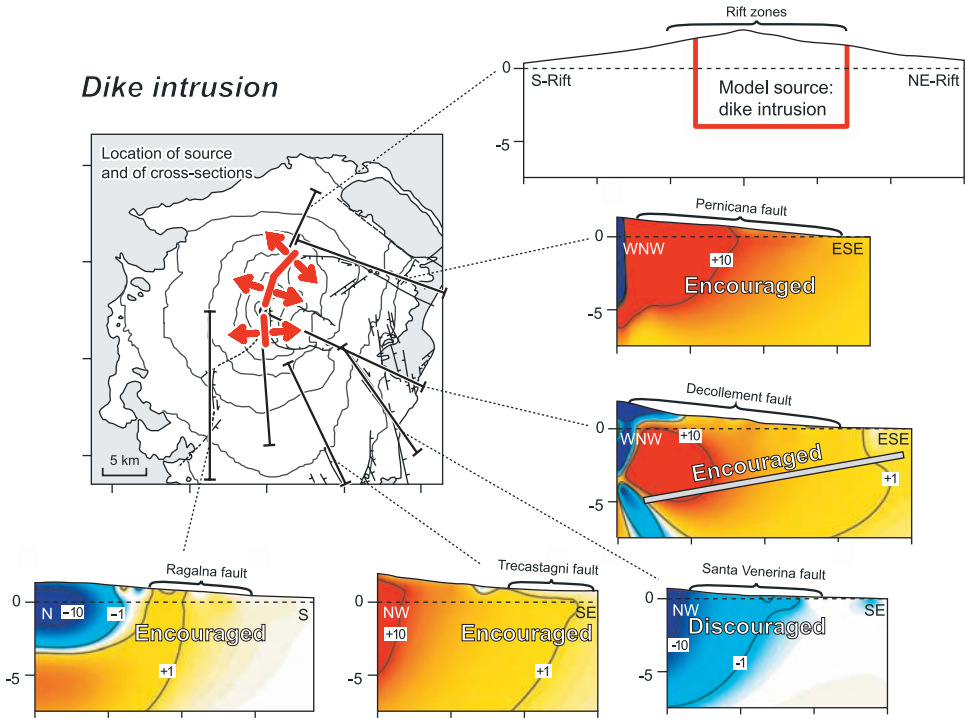


**Figure 5.** Stress changes due to magma intrusion events at Mount Etna: dike intrusion at the rift zones. Positive values (reds), faulting is encouraged, and negative values (blues), faulting is discouraged. See Figure 4 caption for illustration details.

failure stress increase (<1 bar). We note that in the northern area of this fault, where our models predict a Coulomb failure stress decrease, no surface fractures occur.

[35] In summary, the models suggest that dike inflation along the NE and south rifts encourages movement of the Pernicana Fault and of the decollement.

### 4.2. Effects of Flank Movement on the Magmatic System and Further Flank Destabilization

[36] Here we examine the effect of fault slip on the magmatic system and the stress change on the other faults. The results are given in Figures 6 and 7.

#### 4.2.1. Decollement Thrust Faulting

[37] Slip of the decollement results in a significant increase of normal stress at the rift zones at depths of 1–4 km bsl (unclamping >10 bars, Figure 6). The models show an increase in Coulomb failure stress along the Pernicana Fault System. An increase in Coulomb failure stress along the Santa Venerina faulting is shown near the surface and below 3 km bsl and a decrease at intermediate depth. The Trecastagni and Ragalna faults experience a slight increase of the Coulomb failure stress.

[38] In summary, the main effect of decollement slip is that it encourages dike intrusion into the rift zones, and movement along the Pernicana Fault (by 10 bars). We will show later (section 4.3.) that it also results in decompression of the magma plumbing system.

#### 4.2.2. Pernicana Left-Lateral Faulting

[39] Displacement of the Pernicana Fault causes unclamping of the rift zones (Figure 7). The maximum unclamping occurs in the upper NE rift zone, between the summit and the westernmost Pernicana Fault. Unclamping at the south rift is predicted only at the northern 3–4 km of the rift zone, being however much less than at the NE rift. The Coulomb failure stress change at the distant decollement fault plane increases slightly (<0.2 bar). The change of the Coulomb failure stress at the Santa Venerina Fault is positive, and reaches more than 1 bar in the upper 2 km. The Trecastagni and the Ragalna faults experience minor changes of the Coulomb failure stress, slightly negative at the Trecastagni Fault and slightly positive at the Ragalna Fault.

[40] In summary, slip along the Pernicana Fault System results in the unclamping of the NE rift and encourages movement along the Santa Venerina Fault.

### 4.3. Stress Change at the Magmatic System Due to Flank Movement

[41] Slip of the eastern flank transfers the stress and may thus also affect the magmatic system. Extension of the shallow plumbing system of Mount Etna may lead to fumarolic or hydrothermal activity, release or growth of bubbles in magma, or induce the influx of new magma into an existing reservoir.

[42] Experimental studies suggest that changes in the fluid pressure in various rock types are determined by changes in the mean stress [*Roeloffs*, 1996]. We now calculate changes in mean stress $\Delta\sigma_M$ by the mean of the normal stresses $\Delta\sigma_M = 1/3\Delta\sigma_{kk}$, where $\Delta\sigma_{kk}$ indicates summation over the diagonal elements of the stress tensor. The results for a vertical line under the summit of Mount

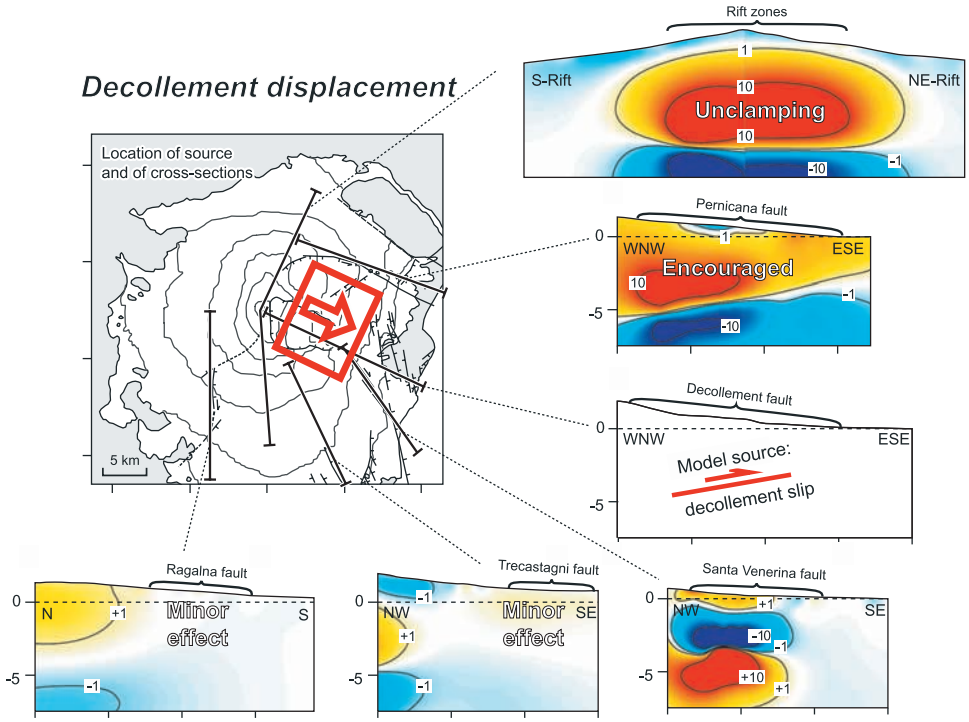


**Figure 6.** Stress changes due to events of faulting during the Mount Etna eastern flank movement: Decollement faulting. Positive values (reds), faulting is encouraged, and negative values (blues), faulting is discouraged. See Figure 4 caption for illustration details.

Etna (the depth ranges from the summit at +3.2 km above sea level to −10 km below sea level) are shown in Figure 8. We refer to $\Delta\sigma_M > 0$ as "compression" and to $\Delta\sigma_M < 0$ as "decompression."

[43] Pernicana faulting and decollement faulting result in decompression at levels from +1 to −6 km depth. This depth is thought to include the bulk of shallow accumulating magma within the Mount Etna edifice. Slip at the Santa Venerina Fault causes only small $\Delta\sigma_M$. Displacements along the Trecastagni and Ragalna faults are associated with even smaller $\Delta\sigma_M$ and not further discussed herein.

[44] In summary, flank movement results in decompression of the shallow magma system.

## 5. Discussion

### 5.1. Volcano-Tectonic Interaction at Mount Etna

[45] The model calculations define three mechanisms of interaction: (1) eruption–flank movement interaction describes how magmatic processes influence flank movement, (2) flank movement–eruption interaction describes how flank movement influences magmatic processes, and (3) fault-fault interaction describes how faults interact within the moving flank (see Figure 9).

#### 5.1.1. Eruption–Flank Movement Interaction

[46] Our models suggest that inflation of a shallow spherical source encourages slip at the deep decollement thrust fault and at the westernmost Pernicana Fault System. Dike opening during the 2002–2003 period encourages fault slip at the decollement and the Pernicana faults (particularly along its westernmost part), explaining the most displacement in the west and the observed eastward propagation.

#### 5.1.2. Flank Movement–Eruption Interaction

[47] The 2002 eruption was preceded by slip on the Pernicana Fault which was associated with an earthquake swarm on September 2002. Our models show that Pernicana Fault movement results in decompression of the shallow reservoir and unclamping of the rift zones. The location of the 2002–2003 eruptive dikes is consistent with the section of the rift zone unclamped by Pernicana and decollement faulting, suggesting that the dike propagation and dike dimension was controlled by flank movement.

[48] We note that just prior to the earthquake swarm, the NE crater was characterized by explosive Strombolian-type eruptions, which ceased immediately after the 22 September Pernicana Fault earthquakes and switched to a mainly effusive eruption type [cf. *Neri et al.*, 2004]. This suggests that flank movement also influenced the eruption dynamics. Our results suggest that the September 2002 earthquake swarm is followed by a change of the eruptive behavior at the NE rift, highlighting a fault-magma interaction. Santa Venerina faulting is discouraged by intrusions considered here.

#### 5.1.3. Fault-Fault Interaction

[49] The faults are arranged in a way so that the decollement fault, the Pernicana Fault and the Santa Venerina Fault are influencing each other. Note that displacement and the related seismic swarms at Santa Venerina indeed commenced after the bulk of slip at block 1, which was consistent with our models of Pernicana slip. Decollement slip mainly increases the stress at the Pernicana Fault, and vice versa.

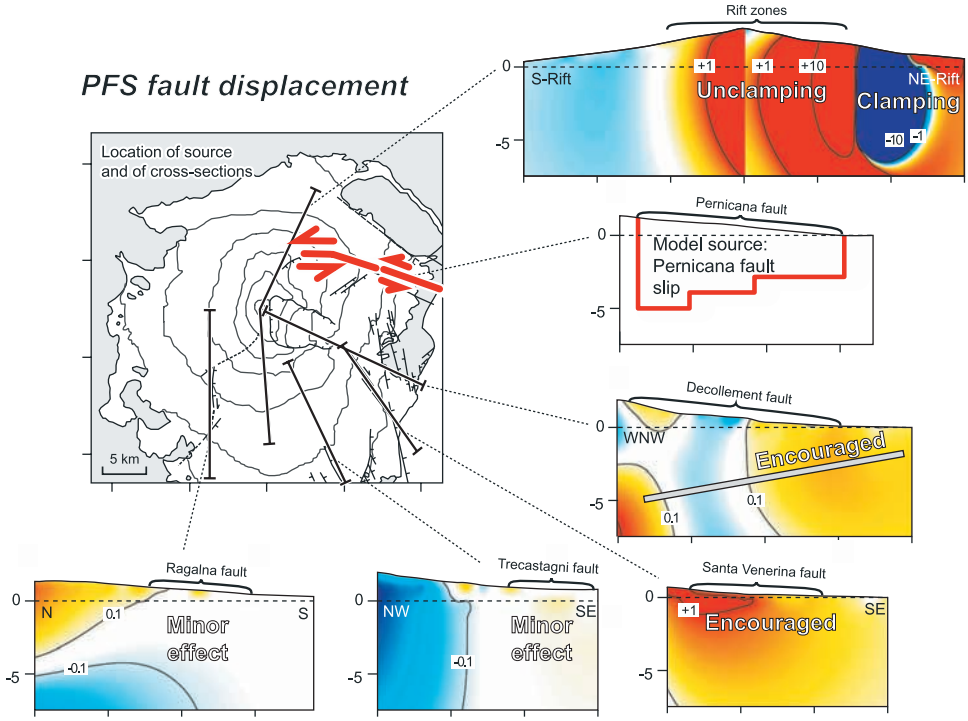


**Figure 7.** Stress changes due to events of faulting during the Mount Etna eastern flank movement: faulting at the Pernicana faults. Positive values (reds), faulting is encouraged, and negative values (blues), faulting is discouraged. See Figure 4 caption for illustration details.

[50] Displacement at the Trecastagni Fault is moderately encouraged (by reservoir inflation, dike intrusion and decollement slip), which is consistent with the seismic swarm and minor surface ruptures observed at the end of November 2002 [*Acocella et al.*, 2003; *Neri et al.*, 2004, 2005]. The destabilization of block 2 is thus directly related to the displacement of block 1 and to magmatic activity.

[51] We also studied effects at the Ragalna Fault, which is essentially locked due to inflation events, but slightly unlocked due to south rift dike intrusion and slip of the northern part of the unstable east flank (Figure 5). This is consistent with the fact that no displacement was observed at Ragalna during the early eruption at the NE rift zone; faulting started after the south rift zone eruption and flank movement [*Rust et al.*, 2005].

### 5.2. Elastic Deformation Mechanics

[52] All our models assume elastic dislocation sources. On the south flank of Kilauea, for example, teleseismic surface waves of the 1975 Kalapana flank movement were interpreted using a landslide model with the associated single force mechanism [*Eissler and Kanamori*, 1987]. A single force could imply that flank movement is entirely gravity-driven and that intrusions into the rift zones occur passively into the newly created void. However, the concept of purely passive intrusions and single force flank movement was refuted by a number of studies, based on the occurrence of forceful dike intrusion with the standard theoretical stress and strain pattern; that is, the intrusion into the Kilauea rift zones compresses the adjacent flanks until this stress is relieved by flank movement and earthquakes [e.g., *Swanson et al.*, 1976; *Dieterich*, 1988; *Dieterich et al.*, 2003]. Also the recent Mount Etna dike intrusions compressed the adjacent flanks and caused typical surface deformation [e.g., *Puglisi et al.*, 2001; *Aloisi et al.*, 2003; *Lundgren et al.*, 2004], suggesting that the conceptual model of elastic dislocation used in this study is also appropriate for Mount Etna.

### 5.3. Regional Tectonics and Remote Stress Field

[53] The magmatic and seismic activity at Mount Etna may be significantly influenced by regional faults and stress fields, which in turn may interact with the local processes studied in this paper. For instance, microseismicity preceding the 2002–2003 eruption of Mount Etna aligned along two regional structural trends oriented NW-SE and NE-SW [*Gambino et al.*, 2004]. The microseismicity clustered at the Mount Etna east flank along NW-SE and NE-SW trends, and at the west flank along a NE-SW trend, generally with dextral focal mechanisms, and interrupted closer to the volcano centre. Because the seismicity increase correlated with geodetic and volcanological evidence of volcano inflation, *Gambino et al.* [2004] suggested that inflation-related stress changes encouraged the preeruptive seismicity, probably coupled to inflation sources at various depths. Our models show that inflation of a shallow magma body centered under Mount Etna slightly decreases shear stress and Coulomb stress at the NW-SE trending fault (compare SV in Figure 4). Those stress changes are largest close to the source and rapidly decline radially, which implies that earthquakes are hindered mainly in the central part of the volcano (the same would apply to the NE-SW trending

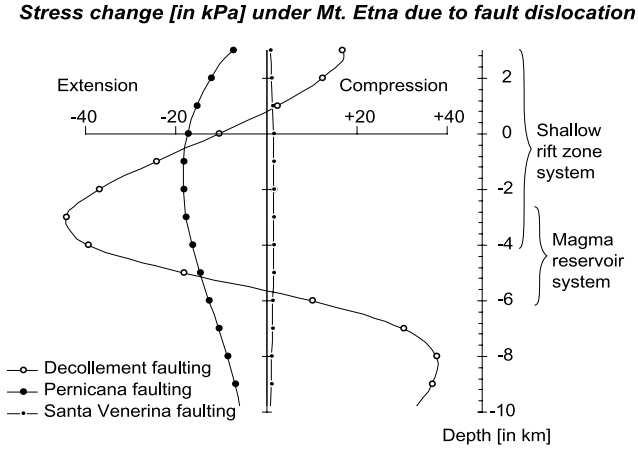


**Figure 8.** Stress change under Mount Etna due to dislocation of the three most important faults: Decollement, Pernicana, and Santa Venerina. A significant stress change occurs only for decollement and Pernicana faulting, which is extensional at the shallow magma system level (magma reservoir and rift zone system).

system if we consider it to be a conjugate trend). These results are thus in agreement with the interruption of seismicity closer to the volcano centre observed by *Gambino et al.* [2004]. However, the pronounced seismicity along the regional trends further away to the east from the volcano centre cannot be explained by the shallow centered source. We conjecture that an inflating magma body that is located at greater depth reduces the normal stress at the regional faults above and may encourage preeruption earthquakes there. A deeper inflation source under the eastern flank as proposed by *Gambino et al.* [2004] can therefore explain preeruptive reactivation of some of the regional structures.

[54] The models of coeruptive flank movement also depend on our understanding of the remote stress conditions. *Gresta et al.* [2005] suggested that dike intrusion associated with the 1981 eruption at the northern Mount Etna flank might have encouraged slip at the Pernicana Fault System, which is consistent with our stress change models for an intruded dike. However, the displacement at the Timpe Fault System (SV in this study) cannot be explained in a homogeneous regional stress field (see negative Coulomb failure stresses at SV in Figure 5). Fault slip there could either be understood by heterogeneous stress tensors on the eastern Etna flank [*Gresta et al.*, 2005], and/or by its coupling to other processes. Our study suggests that the Santa Venerina Fault is coupled to block 1 movement in the north, and not so much to shallow level intrusions.

### 5.4. External Triggering of Mount Etna Flank Eruptions

[55] Volcanic activity and flank movement at Mount Etna appear to be mutually interacting processes. As shown in this article, magma intrusions increase the stress at active faults and encourage further flank movement. On the other side, flank movement causes stress changes at the magmatic system and encourages dike intrusions. Nevertheless, the exact mechanism pertaining to how flank movement influences or even triggers intrusions or eruptions is still not clear. The transfer of stress may have consequences on the mechanics and on the magma-physical dynamics of the volcano, which are most likely interrelated. Flank movement results in decompression of present magma reservoirs (Figure 8). Bubbles may increase, be released or newly formed and increase substantially in size during ascent, what may lead to an eruption [*Linde and Sacks*, 1998]. Other effects may be related to the convection dynamics of magma bodies or rectified diffusion [see *Hill et al.*, 2002, and references therein]. The direct mechanical effects of flank movement at Mount Etna are unclamping of the rift zones, fracture opening and hence the facilitation of magma dike propagation [see also *Kilburn*, 2003]. We showed this via the normal stress computations along the rift zones.

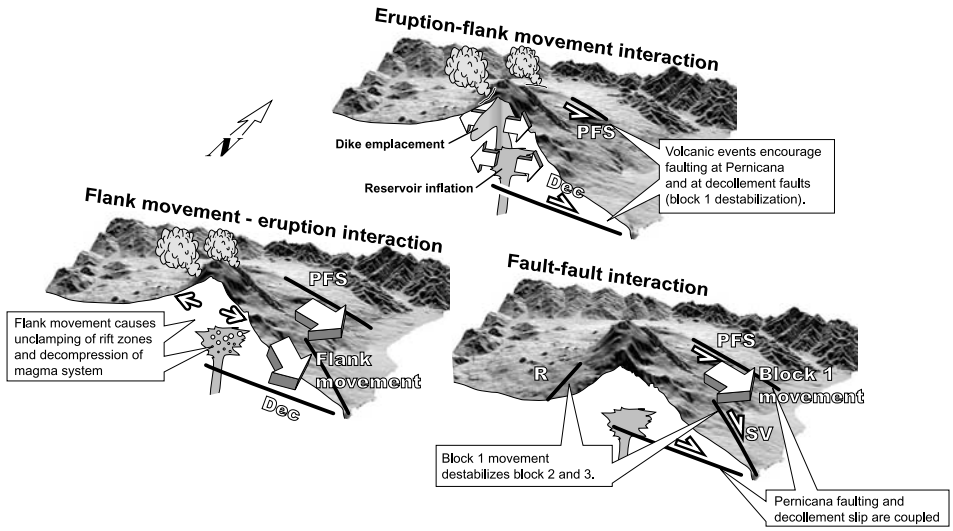


**Figure 9.** Sketch exemplifying the three modes of interaction evidenced at Mount Etna between the volcano and the faults as proposed in this study. Cross section is east-west.

Movement of the Mount Etna eastern flank caused unclamping of those parts of the rift zones which erupted during the 2002–2003 events. The models suggest that most of the unclamping occurred within the upper 5–7 km of the edifice with a maximum at or close to a central reservoir/conduit system (Figures 6 and 7). In these cases, lateral propagation of magma above 5–7 km depth is likely, causing lateral propagating fissures. *Acocella and Neri* [2003] and *Neri et al.* [2005] suggest that peripheral eruptions occur occasionally on the flanks of the volcano, controlled by the reactivation of (hidden) crustal fracture zones. Stress changes due to shallow flank movement may make such dike propagation into preexisting structures possible.

### 5.5. Feedback Processes Between Flank Movement and Magmatic Events

[56] The numerical models suggest that magmatic activity (inflation of a reservoir and emplacement of dikes) encourages motion of the eastern flank, which, in turn, encourages the rise of magma to shallower levels within the volcano. These results therefore explain the mutual interaction between magmatic events and flank instability during the 2002–2003 eruption. Our study confirms a phenomenon that was understood hitherto on a mostly qualitative level [e.g., *McGuire et al.*, 1990; *Borgia et al.*, 1992]. Our study suggests that the volcano-tectonic feedback consists of three mutually enhancing processes: (1) magma chamber inflation, (2) flank movement, and (3) dike intrusion and eruption.

[57] Similar feedback processes have probably occurred in the past. For example, after the 1983 eruption, Etna inflated until 1986; the slip of the flank at the Pernicana Fault was observed during the 1984–1988 period and the eruptions occurred in 1985 and 1987 [*Neri et al.*, 2005]. The recent history of Etna may be interpreted in terms of recurring episodes of feedback between magma emplacement and flank instability.

## 6. Conclusions

[58] We studied the stress transfer associated to the events of the Etna 2002–2003 eruptive sequence. Using three-dimensional numerical models, we calculated stress changes related to shallow reservoir inflation, dike intrusion and fault displacement. Our models suggest three mechanisms of interaction acting at Mount Etna. Static stress changes provide an explanation of how magmatic activity encourages flank movement, how flank movement encourages magmatic activity, and how faulting at the unstable flanks triggers further faulting. The application of the numerical models to the main events characterizing the 2002–2003 eruption suggests the following points:

[59] 1. The inflation of the volcano induces the slip of its eastern flank along the Pernicana Fault System and the décollement.

[60] 2. The movement of the volcano east flank may induce or enhance the emplacement of dikes mainly along the NE rift and also along the south rift. The faults are interacting and the area involved in flank movement increases further to the south, incorporating the Trecastagni and Santa Venerina fault zones.

[61] 3. The opening of the NE and the south rifts may induce further slip along the decollement at the base of the unstable flank, along the Pernicana Fault and along the Trecastagni Fault. These results confirm the existence of a feedback process between flank movement and magmatic activity at Etna during the 2002–2003 eruption.

[62] **Acknowledgments.** We thank Dave Pollard and the "Stanford Rock Fracture Project" for providing Poly3d and Paul Lundgren for his debugging efforts and further help with the modeling technique. We appreciate constructive reviews by Jim Dieterich, Peter Cervelli, and the Associate Editor. This study was supported by grant WA1642 from the German Research Foundation (Deutsche Forschungsgemeinschaft) awarded to T.R.W.

## References

Acocella, V., and M. Neri (2003), What makes flank eruptions? The 2001 Etna eruption and its possible triggering mechanisms, *Bull. Volcanol.*, *65*, 517–529.

Acocella, V., and M. Neri (2005), Structural features of an active strike-slip fault on the sliding flank of Mount Etna (Italy), *J. Struct. Geol.*, *27*(2), 343–355.

Acocella, V., B. Behncke, M. Neri, and S. D'Amico (2003), Link between major flank slip and 2002–2003 eruption at Mount Etna (Italy), *Geophys. Res. Lett.*, *30*(24), 2286, doi:10.1029/2003GL018642.

Aloisi, M., A. Bonaccorso, S. Gambino, M. Mattia, and G. Puglisi (2003), Etna 2002 eruption imaged from continuous tilt and GPS data, *Geophys. Res. Lett.*, *30*(23), 2214, doi:10.1029/2003GL018896.

Azzaro, R. (2004), Seismicity and active tectonics in the Etna region: Constraints for a seismotectonic model, in *Mt. Etna: Volcano Laboratory*, *Geophys. Monogr. Ser.*, vol. 143, edited by A. Bonaccorso et al., pp. 205–220, AGU, Washington, D. C.

Becker, A. A. (1992), *The Boundary Element Method in Engineering*. McGraw-Hill, New York.

Beeler, N. M., R. W. Simpson, D. A. Lockner, and S. H. Hickman (2000), Pore fluid pressure, apparent friction and Coulomb failure, *J. Geophys. Res.*, *105*, 25,533–25,554.

Behncke, B., and M. Neri (2003), Cycles and trends in the recent eruptive behavior of Mount Etna, *Can. J. Earth Sci.*, *40*, 1405–1411.

Behncke, B., M. Neri, and A. Nagay (2005), Lava flow hazard at Mount Etna (Italy): New data from a GIS-based study, in *Kinematics and Dynamics of Lava Flows*, edited by M. Manga and G. Ventura, *Spec. Pap. Geol. Soc. Am.*, *396–13*, 187–205, doi:10.1130/2005.2396(13).

Bonforte, A., and G. Puglisi (2003), Magma uprising and flank dynamics on Mount Etna volcano, studied using GPS data (1994–1995), *J. Geophys. Res.*, *108*(B3), 2153, doi:10.1029/2002JB001845.

Borgia, A., L. Ferrari, and G. Pasquarè (1992), Importance of gravitational spreading in the tectonic and volcanic evolution of Mount Etna, *Nature*, *357*, 231–235.

Borgia, A., P. T. Delaney, and R. P. Denlinger (2000), Spreading volcanoes, *Annu. Rev. Earth Planet. Sci.*, *28*, 539–570.

Branca, S., D. Carbone, and F. Greco (2003), Intrusive mechanism of the 2002 NE-Rift eruption at Mt. Etna (Italy) inferred through continuous microgravity data and volcanological evidences, *Geophys. Res. Lett.*, *30*(20), 2077, doi:10.1029/2003GL018250.

Branca, S., M. Coltelli, and G. Groppelli (2004), Geological evolution of Etna Volcano, in *Mt. Etna: Volcano Laboratory*, *Geophys. Monogr. Ser.*, vol. 143, edited by A. Bonaccorso et al., pp. 49–63, AGU, Washington, D. C.

Burton, M., M. Neri, and D. Condarelli (2004), High spatial resolution radon measurements reveal hidden active faults on Mt. Etna, *Geophys. Res. Lett.*, *31*(7), L07618, doi:10.1029/2003GL019181.

Calvari, S., L. H. Tanner, G. Groppelli, and G. Norini (2004), Valle del Bove, eastern flank of Etna volcano: a comprehensive model for the opening of the depression and implications for future hazards, in *Mt. Etna: Volcano Laboratory*, *Geophys. Monogr. Ser.*, vol. 143, edited by A. Bonaccorso et al., pp. 65–75, AGU, Washington, D. C.

Comninou, M. A., and J. Dundurs (1975), The angular dislocation in a half-space, *J. Elast.*, *5*, 203–216.

Corsaro, R. A., M. Neri, and M. Pompilio (2002), Paleo-environmental and volcano-tectonic evolution of the south-eastern flank of Mount Etna during the last 225 ka inferred from volcanic succession of the Timpe, Acireale, Sicily, *J. Volcanol. Geotherm. Res.*, *113*, 289–306.

Crouch, S. L., and A. M. Starfield (1983), *Boundary Element Methods in Solid Mechanics: With Applications in Rock Mechanics and Geological Engineering*, Allen and Unwin, St. Leonards, N.S.W., Australia.

Dieterich, J. H. (1988), Growth and persistence of Hawaiian volcanic rift zones, *J. Geophys. Res.*, *93*, 4258–4270.

Dieterich, J. H., V. Cayol, and P. G. Okubo (2003), Stress changes prior to and during the Pu'u'Ö'ö-Kupaianaha eruption of Kilauea volcano, *U.S. Geol. Surv. Prof. Pap.*, *1676*, 187–201.

Eissler, H. K., and H. Kanamori (1987), A single-force model for the 1975 Kalapana, Hawaii earthquake, *J. Geophys. Res.*, *92*, 4827–4836.

Gambino, S., A. Mostaccio, D. Patanè, L. Scarfì, and A. Ursino (2004), High-precision locations of the microseismicity preceding the 2002–2003 Mt. Etna eruption, *Geophys. Res. Lett.*, *31*, L18604, doi:10.1029/2004GL020499.

Gresta, S., F. Ghisetti, E. Privitera, and A. Bonanno (2005), Coupling of eruptions and earthquakes at Mt. Etna (Sicily, Italy): A case study from the 1981 and 2001 events, *Geophys. Res. Lett.*, *32*, L05306, doi:10.1029/2004GL021479.

Harris, R. A. (1998), Introduction to a special section: Stress triggers, stress shadows, and implications for seismic hazards, *J. Geophys. Res.*, *103*, 24,347–24,358.

Hill, D. P., F. Pollitz, and C. Newhall (2002), Earthquake-volcano interactions, *Phys. Today*, *55*(11), 41–47.

Kilburn, C. R. J. (2003), Multiscale fracturing as a key to forecasting volcanic eruptions, *J. Volcanol. Geotherm. Res.*, *125*, 271–289.

Linde, A. T., and I. S. Sacks (1998), Triggering of volcanic eruptions, *Nature*, *395*, 888–890.

Lo Giudice, E., G. Patane, R. Rasa, and R. Romano (1982), The structural framework of Mount Etna, *Mem. Soc. Geol. It.*, *23*, 125–158.

Lundgren, P., P. Berardino, M. Coltelli, G. Fornaro, R. Lanari, G. Puglisi, E. Sansosti, and M. Tesauro (2003), Coupled magma chamber inflation and sector collapse slip observed with synthetic aperture radar interferometry on Mt. Etna volcano, *J. Geophys. Res.*, *108*(B5), 2247, doi:10.1029/2001JB000657.

Lundgren, P., F. Casu, M. Manzo, A. Pepe, P. Berardino, E. Sansosti, and R. Lanari (2004), Gravity and magma induced spreading of Mount Etna volcano revealed by satellite radar interferometry, *Geophys. Res. Lett.*, *31*, L04602, doi:10.1029/2003GL018736.

Marzocchi, W., E. Casarotti, and A. Piersanti (2002), Modeling the stress variations induced by great earthquakes on the largest volcanic eruptions of the 20th century, *J. Geophys. Res.*, *107*(B11), 2320, doi:10.1029/2001JB001391.

McGuire, W. J., A. D. Pullen, and S. J. Saunders (1990), Recent dyke-induced large-scale block movement at Mount Etna and potential slope failure, *Nature*, *343*, 357–359.

Murru, M., C. Montuori, M. Wyss, and E. Privitera (1999), The locations of magma chambers at Mt. Etna, Italy, mapped by *b*-values, *Geophys. Res. Lett.*, *26*, 2553–2556.

Neri, M., V. Acocella, and B. Behncke (2004), The role of the Pernicana Fault System in the spreading of Mount Etna (Italy) during the 2002–2003 eruption, *Bull. Volcanol.*, *66*, 417–430.

Neri, M., V. Acocella, B. Behncke, V. Maiolino, A. Ursino, and R. Velardita (2005), Contrasting triggering mechanisms of the 2001 and 2002–2003 eruptions of Mount Etna (Italy), *J. Volcanol. Geotherm. Res.*, *144*, 235–255.

Nostro, C., R. S. Stein, M. Cocco, M. E. Belardinelli, and W. Marzocchi (1998), Two-way coupling between Vesuvius eruptions and southern Apennine earthquakes, Italy, by elastic stress transfer, *J. Geophys. Res.*, *103*, 24,487–24,504.

Patanè, D., P. De Gori, C. Chiarabba, and A. Bonaccorso (2003), Magma ascent and the pressurization of Mount Etna's volcanic system, *Science*, *299*, 2061–2063.

Puglisi, G., A. Bonforte, and S. R. Maugeri (2001), Ground deformation patterns on Mount Etna, 1992 to 1994, inferred from GPS data, *Bull. Volcanol.*, *62*, 371–384.

Roeloffs, E. (1996), Poroelastic techniques in the study of earthquake related hydrologic phenomena, *Adv. Geophys.*, *37*, 135–196.

Rust, D., and M. Neri (1996), The boundaries of large-scale collapse on the flanks of Mount Etna, Sicily, in *Volcano Instability on the Earth and Other Planets*, edited by W. C. McGuire, A. P. Jones, and J. Neuberg, *Geol. Soc. Spec. Publ.*, *110*, 193–208.

Rust, D., B. Behncke, M. Neri, and A. Ciocanel (2005), Nested zones of instability in the Mount Etna volcanic edifice, Italy, *J. Volcanol. Geotherm. Res.*, *144*, 137–153.

Siebert, L. (1992), Threats from debris avalanches, *Nature*, *356*, 658–659.

Stein, R. S. (1999), The role of stress transfer in earthquake occurrence, *Nature*, *402*, 605–609.

Swanson, D. A., W. A. Duffield, and R. S. Fiske (1976), Displacement of the south flank of Kilauea Volcano: The result of forceful intrusion of magma into the rift zones, *U.S. Geol. Surv. Prof. Pap.*, *963*, 39 pp.

Tanaka, S., M. Ohtake, and H. Sato (2004), Tidal triggering of earthquakes in Japan related to the regional tectonic stress, *Earth Planets Space*, *56*, 511–515.

Thatcher, W., and J. C. Savage (1982), Triggering of large earthquakes by magma-chamber inflation, Izu Peninsula, Japan, *Geology*, *10*, 637–640.

Thomas, A. L. (1993), Poly3D: A three-dimensional, polygonal element, displacement discontinuity boundary element computer program with applications to fractures, faults, and cavities in the Earth's crust, M. S. thesis, Stanford Univ., Stanford, Calif.

Tibaldi, A., and G. Groppelli (2002), Volcano-tectonic activity along structures of the unstable NE flank of Mount Etna (Italy) and their possible origin, *J. Volcanol. Geotherm. Res.*, *115*, 277–302.

Voight, B., H. Glicken, R. J. Janda, and P. M. Douglas (1981), Catastrophic rockslide avalanche of May 18, in *The 1980 Eruptions of Mount St. Helens, Washington*, edited by P. W. Lipman and D. R. Mullineaux, *U.S. Geol. Surv. Prof. Pap.*, *1250*, 347–377.

Walter, T. R., and F. Amelung (2004), Influence of volcanic activity at Mauna Loa, Hawaii, on earthquake occurrence in the Kaoiki Seismic Zone, *Geophys. Res. Lett.*, *31*, L07622, doi:10.1029/2003GL019131.

Walter, T. R., V. Troll, B. Cailleau, A. Belousov, H.-U. Schmincke, P. Bogaard, and F. Amelung (2005), Rift zone reorganization through flank instability on ocean island volcanoes: Tenerife, Canary Islands, *Bull. Volcanol.*, *67*, 281–291.

V. Acocella, Dipartimento di Scienze Geologiche, Università di Roma TRE, L. S. L. Murialdo, 1, Rome, I-00146, Italy.

F. Amelung, Marine Geology and Geophysics, Rosenstiel School of Marine and Atmospheric Science, University of Miami, 4600 Rickenbacker Causeway, Miami, FL 33149, USA.

M. Neri, Istituto Nazionale di Geofisica e Vulcanologia, Sezîone di Catania Piazza Roma, 2, I-95123, Catania, Italy.

T. R. Walter, VolcanoTectonics Lab, Section 2.1 Natural Disasters, GeoForschungsZentrum (GFZ), Telegrafenberg, D-14473, Potsdam, Germany. (twalter@gfz-potsdam.de)